Proceedings of the Third International Conference

ADVANCES IN NUMERICAL METHODS AND APPLICATIONS

$$\mathcal{O}(h^3)$$

Sofia, Bulgaria 21 – 26 August 1994

Editors

I. T. Dimov

Bl. Sendov

P. S. Vassilevski

Bulgarian Academy of Sciences

World Scientific

Singapore • New Jersey • London • Hong Kong

Numerical Approach to Ideal Separation on Airfoils. Application of Deformed Quasi-Parabolic Coordinates

M. D. Todorov C. I. Christov*

Abstract

The notion of discontinuous ideal flow consisting of potential streaming and stagnation zone (Helmholtz-Kirchhoff scheme) is applied for modelling the flow around airfoils. Deformed quasi-parabolic coordinates are introduced and difference schemes are devised for Laplace equation and for the equation for shape function of the free boundary. An iterative procedure is employed for defining the separation point. The performance of the numerical technique is displayed on NACA2412 airfoil. Results are presented for two angles of attack (8° and 16°). The pressure distributions on the lower and upper surfaces of airfoil compare quantitatively very well with the experimental data. The predictions for the drag and lifting forces are also in very good agreement (about 95%) with the experimentally measured values.

1 Introduction

Despite the numerous publications (see, e.g., [9] for the classical works), the investigation of inviscid flows with separation not only retains its actuality, but gathers some new impetus because of the quest for the limiting solutions of Navier-Stokes equations for large Reynolds numbers ([14, 12]). The problem is that $Re \to \infty$ yields singular asymptotic problem and the so-called "inner solution" can not be matched to the potential solution for the ideal flows around bluff bodies. In these flows, the boundary layer separates and violates the main assumptions of "inner in asymptotic sense" solution. The singular asymptotic nature of Navier-Stokes equations for vanishing viscosity (large Reynolds numbers) dictates that the "outer" solution must be of more complex nature than the mere potential flow.

*On leave from the National Institute of Meteorology and Hydrology, Bulgarian Academy of Sciences, Sofia, Bulgaria

Another candidate for an "outer" solution appears to be the Helmholtz-Kirchhoff separated inviscid flow introduced first by Helmholtz [10]. The Helmholtz model consists of potential and stagnation zones that match at prior unknown free stream line (tangential discontinuity). The free stream line originates at the body in a point called "detachment" or "separation" point. When the body has sharp edges, the position of detachment point is one of these edges and then the method of hodograph, as employed by Kirchhoff [11], was higly efficient for solving the separation problem. For bluff bodies, however, the problem of detachment point hindered the development of the techniques for solution. A condition [17] for smooth separation (called "condition of Brillouin-Villat") was established to determine the position of separation. Brodetsky [2] was the first to find an approximate solution to the problem of circular cylinder with Brillouin-Villat condition acknowledged.

The problem with Brodetsky's solution is that it predicts a very early separation of the flow (around 55° from the leading stagnation point), while the experiments show a value of order of 80°. In our opinion, this unsatisfactory result can be explained by the rough approximation of the Brodetsky method. He used only three terms in the Lorain series for approximate representation of the conformal mapping in the framework of hodograph method. Recently the authors [3, 4, 5] revisited numerically the Helmholtz-Kirchhoff-Brodetsky problem (the separated flow around circular cylinder). A finite-differences method was used with a specially devised algorithm for iterative determination of detachment point. It was found that the separation point is at 78° which differed significantly from Brodetsky's result being much closer to the experimental measurements and to the high-Re direct numerical simulations [7, 8] in which the separation angle was 95°. In [15] another solution to the same problem was developed, based on the integral-equations method and with similar iterative algorithm for defining the detachment point. The integral-equations method confirmed quantitatively the results of the finite-difference method.

The finite-difference algorithm was also applied to the ideal separated flow around airfoils [16, 6] and encouraging results were obtained for airfoils from the series of NACA. The purpose of the present work is to enhance the efficiency of the said numerical scheme by means of introducing a specially devised quasi-parabolic coordinates that are topologically most suited to the geometry of the flow around airfoils at considerable angle of attack.

2 Quasi-Parabolic Coordinates

In our previous works concerned with the circular-cylinder flow, we used parabolic coordinates since they are better suited to describe stagnation zones extending to infinity. In [16] we applied the parabolic coordinates to the separated flow around airfoil, as well, but part of the advantages of the parabolic coordinates were lost when the flow had non-trivial angle of attack. Then one faces the choice to orient the parabolic coordinates either along the chord of profile (the horizontal part of

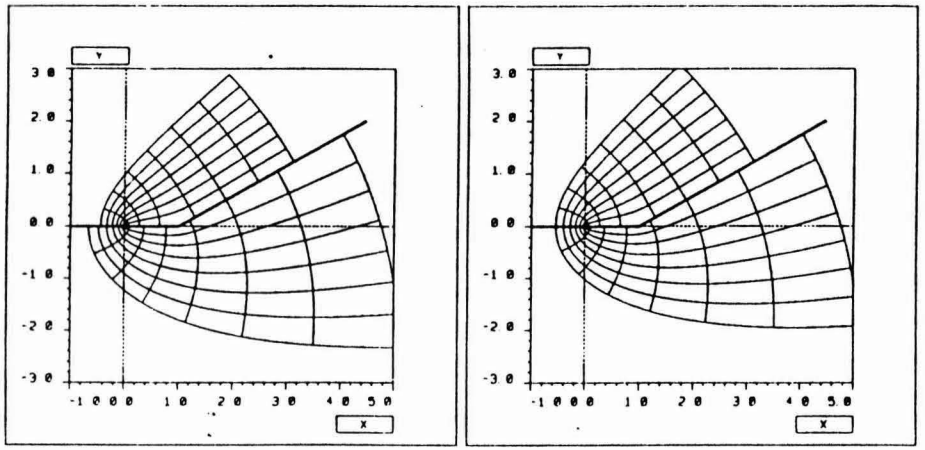

Figure 1: Left: the parabolic coordinates in the upper and lower regions. Right: quasi-parabolic coordinates in the whole region.

the thick line in Fig. 1) or along the direction of the flow (the inclined part of the thick line in Fig. 1). The former case yields a naturally dense mesh in the vicinity of the leading point of the airfoil where the good resolution is badly needed but then the asymptotic behaviour of the free lines is not the one of a coordinate line. The latter case is attractive because in it the asymptotic behaviour of separation lines is conveniently expressed as approaching some constants at infinity. When the constants are different from zero one has a parabolically expanding zone (Kirchhoff's solution). When both the asymptotic constants are equal to zero - a cusped zone is modelled. Due to the specifics of our algorithmic implementation we had to opt in [16] for the parabolic coordinates that were oriented with the direction of the flow. This forced us to introduce significantly nonuniform mesh in the vicinity of the leading point of the airfoil in order to capture the behaviour of the flow there. Here we combine the advantages of the two approaches by means of quasi-parabolic coordinate system.

Consider the upper and lower regions (above and bellow the thick line in Fig. 1, respectively) into which the whole region is divided by the chord and the direction of flow. These regions are subjected to conformal mappings rendering them into the upper and lower half-planes of the transformed region. Thus the thick line becomes a straight line. Note that the upper region in the physical plane is bounded by an angle lesser than 2π, while the lower region - by an angle larger than 2π. Let us denote now by $\omega_\mp$ the respective half-plane in the transformed region and by $z_\mp$ - the original region(s), i.e., $x_\mp = \mathbf{Re}[z_\mp]$, $y = \mathbf{Im}[z_\mp]$. The sign "$-$" refers to the upper half-plane, and the sign "$+$" - to the lower. Then for the inverse transformation of the

two conformal mappings we have

$$z_\mp = r_\mp^{\frac{\pi\mp\alpha}{\pi}} \exp\left[i\left(\frac{\pi\mp\alpha}{\pi}\theta_\mp + \alpha\right)\right], \qquad r_\mp = \sqrt{\xi_\mp^2 + \zeta_\mp^2}, \quad \theta_\mp = \arctan\frac{\zeta_\mp}{\xi_\mp}. \tag{1}$$

Here $\xi_\mp$ and $\zeta_\mp$ are the variables in the transformed region(s).

It is interesting to note that the above defined coordinate system ξ, ζ is orthogonal and its two metric coefficients are equal, say $Q(\xi,\zeta) \equiv g^{11} = g^{22}$. The Laplace equation for the stream function and the modulus of the velocity adopt the following simple forms

$$\frac{1}{Q(\xi,\zeta)}(\psi_{\xi\xi} + \psi_{\zeta\zeta}) = 0. \qquad |\nabla\psi|^2 \equiv \frac{1}{Q(\xi,\zeta)}(\psi_\xi^2 + \psi_\zeta^2). \tag{2}$$

Now we introduce a local parabolic coordinate system $O\sigma_\mp\tau_\mp$ in each of the half-planes of the transformed plane, namely

$$\xi_\mp = \frac{1}{2}(\tau_\mp^2 - \sigma_\mp^2) - X_0, \quad \sigma_\mp \geq 0; \qquad \zeta_\mp = \sigma_\mp\tau_\mp, \quad -\infty < \tau_+ < 0, \quad 0 < \tau_- < \infty. \tag{3}$$

Here X_0 is the focal point of the parabolic coordinates. Without this parameter the focal point of parabolic coordinates would have been at the vertex of the angle between the chord and direction of the flow. Without loosing the generality we can set it equal to unity, since we use it as the characteristic scale when rendering the problem dimensionless. Practically speaking, X_0 is the focal point of the parabola fitting best the leading edge of the airfoil under consideration, i.e., the characteristic length X_0 is slightly shorter than the chord L.

The two parabolic coordinate systems defined by (3) are different in the two half-planes (see the left part of Fig. 1). However, they can be matched along the line $\tau_\mp = 0$ (or which is the same for $-\infty < \xi_\mp < -1$). If a new σ-coordinate common for the two systems is introduced, namely

$$\frac{\sigma_\mp^4}{4} + \sigma_\mp^2 + 1 = \left(\frac{\sigma^4}{4} + \sigma^2 + 1\right)^{\frac{\pi}{\pi\mp\alpha}} \quad \text{or} \quad \sigma_\mp = \sqrt{\left|\sigma^2 + 2\right|^{\frac{\pi}{\pi\mp\alpha}} - 2} \tag{4}$$

If one defines the new τ-coordinate in the upper and lower half-plane respectively as $\tau \equiv \tau_-$ or $\tau \equiv \tau_+$ one gets the coordinate system, depicted in the right part of Fig. 1. Note that after the introduction of the new σ-coordinate the two parabolic coordinate systems do not match neither on the chord nor on the cut behind the body and that is why the quasi- parabolic coordinates are discontinuous (across the thick line in Fig. 1. This is not a problem, because the stream function is not supposed to be continuous when crossing the thick line. Physically, the flows in the two regions do not interact with each other. In a sense they are screened by the chord and by the cut (the separation lines).

In the practical implementation of the quasi-parabolic coordinates QPC we prefer not to introduce the transformation (4) into the governing equations since it would lead us to variable coefficient in the operator in Laplace equation responsible for the σ second-derivative. The other way around is to keep in mind when defining the difference function approximating the stream function that when crossing the line $\tau_{\mp} = 0$ we have to match difference functions with different σ number. Of course, this is possible only because both parabolic systems that comprise our QPC system are orthogonal to the said τ-line. Moreover, even after the transformation (4) they remain orthogonal.

Furthermore we omit the indices $\mp$ of ξ and η or σ and τ. They will be explicitly referred to only in the places where confusion may arise.

3 Posing the problem

In order to render the computational domain to a region with fixed boundaries we introduce scaled coordinates

$$\eta = \frac{\sigma - S}{S_\infty - S}\,, \quad \tau = \tau\,; \qquad S_\infty = \frac{\sqrt{2}x_\infty}{\sqrt{x_\infty} + \tau} \tag{5}$$

where x_∞ is an appropriately chosen parameter called "actual infinity". Transformation (5) renders the physical region of the flow into the strip $[0 \le \eta \le 1\,,\ -\infty < \tau < \infty]$ of the computational domain. The advantage of (5) over the transformations with $S_\infty = const$ is that for $\tau \to \infty$, it gives $S_\infty \to 0$, i.e., the outer boundary of the region shrinks at infinity behind the body. Thus the excessive coarseness of the η-grid at large distances behind the body can be avoided. In terms of the scaled variables (η, τ), the Laplace equation for the stream function adopts the form

$$a\psi_{\eta\eta} - 2b\psi_{\eta\tau} + \psi_{\tau\tau} + d\psi_\eta = 0\,,$$

$$a = \frac{1 + (\eta(S' - S'_\infty) - S')}{(S_\infty - S)^2}\,, \quad b = \frac{S' - \eta(S' - S'_\infty)}{S_\infty - S}\,, \tag{6}$$

$$d = \frac{-S'' + \eta(S'' - S''_\infty)}{S_\infty - S} + \frac{[S' - \eta(S' - S_\infty)](S'_\infty - S')}{(S_\infty - S)^2}\,.$$

This equation is solved with the boundary conditions

$$\psi|_{\eta=0} = 0\,, \quad \psi|_{\tau\to\pm\infty} \approx U_\infty[S + \eta(S_\infty - S)]\tau \tag{7}$$

The first one acknowledges the fact that boundary of the composite region "body / stagnation zone" is a stream line. The second one gives the asymptotic behaviour at infinity of the undisturbed flow.

The dynamic condition (Bernoulli integral) now becomes an explicit equation for the shape function $S(\tau$ of the free boundary and reads

$$\frac{1}{(S_\infty - S)^2(S^2 + \tau^2)}(1 + S'^2)\left[\frac{\partial\psi}{\partial\eta}\Big|_{\eta=0}\right]^2 = 1\,, \quad \text{for} \quad \tau_u^* \le \tau\,, \tau_l^* \ge \tau\,. \tag{8}$$

where τ_l^* and τ_u^* are the coordinates of the detachment points, respectively on the lower and upper surfaces of airfoil. Thus the b.v.p. to be solved is completed.

For the drag and lifting-force coefficients one has

$$C_x = \int_{-\tau_1}^{\tau_1} p(S + S'\tau)\,d\tau\,, \qquad C_y = \int_{-\tau_1}^{\tau_1} p(SS' - \tau)\,d\tau$$

where p is the dimensionless pressure.

4 Numerical Implementation

We use in τ-direction $N_1 = N + 2N_W$ nodes and introduce a mesh which is non-uniform both over the chord (the first N points) of profile and over the two "shores" of the cut (the other $2N_W$ points).

Here we do not discuss in detail the difference approximation to Laplace equation for stream function. It is similar to [3, 4, 16] and makes use of splitting method as an iterative procedure. The scheme for the Bernoulli integral is of second order of approximation. In the upper half-plane of the flow the approximation is as follows.

$$\hat{S}_{j+1}^{k+1} - \hat{S}_j = \pm g_{j+1}\sqrt{\frac{\left[2S_\infty^{j+\frac{1}{2}} - \left(\hat{S}_j + S_{j+1}^{\alpha,k}\right)\right]^2\left[\left(\hat{S}_j + \hat{S}_{j+1}^k\right)^2 + (\tau_j + \tau_{j+1})^2\right]}{4\left(T_j^\alpha + T_{j+1}^\alpha\right)^2}} - 1\,, \tag{9}$$

for $j = j_u^*, \ldots, N$. It is similar in the lower part but the calculations are conducted for $j = j_l^*, \ldots, 1$. j_u and j_l are the indices of the detachment points on the upper and lower airfoil surface, respectively. For the sake of brevity is denoted

$$S_\infty^{j\pm\frac{1}{2}} = \frac{2\sqrt{2}x_\infty}{2\sqrt{x_\infty} + (\tau_j + \tau_{j\pm1})}$$

The scheme (9) requires inlet condition $\hat{S}_{j_u^*} = S_{j_u^*}^B$, where $S^B(\tau)$ is the known shape function of the rigid boundary. Then at each point internal iterations are conducted (referred by the index k) until convergence and thus the value $\hat{S}_j$ is obtained as a solution of the nonlinear difference equation.

The algorithm requires also a global iteration. Let us denote by S^α the shape function on the current iterative stage. Having S^α prescribed we solve the Laplace

equation. Thus the "new" values for $\psi^{\alpha+1}$ are obtained. Then we calculate the quantity $\psi_\eta|_{\eta=0}$ and then solve the difference approximation of (9) and obtain a prediction for the shape function $\hat{S}(\tau)$. The strongly coupled character of the model requires some measures for preventing instability. The simplest one is to introduce relaxation for S according to the standard formula with the only difference that the relaxation parameter ω_j is taken here to be a function of the point, namely

$$S_j^{\alpha+1} = \omega_j \hat{S}_j + (1-\omega_j) S_j^\alpha \ ,$$

$$\omega_j \equiv \frac{\tau_2}{\tau_2 + \epsilon_{rj}} \ , \ \epsilon_{rj} = \frac{\hat{S}_j - S_j^\alpha}{\hat{S}_j} \quad \text{for} \quad j = j_u^*, \ldots, N_1 \ ; \quad j = 1, \ldots, j_l^* \qquad (10)$$

Our numerical experiments show that the optimal values for the "overall" relaxation parameter τ_2 lie in the interval $0.01 \leq \tau_2 \leq 0.05$. The criterion for terminating the global iteration is $\max \left| (\hat{S}_j - S_j^\alpha)/\hat{S}_j \right| \leq 10^{-4}$

5 Results and Discussion

We have performed numerical tests with different angles of attack for the airfoil NACA2412 for whose shape there exists analytical representation, and for which comprehensive experimental data can be found in the literature, as well.

For $x_\infty = 20$, the pressure on the free surface is smaller than 10^{-3}, i.e. on such distances the calculated flow velocity is virtually equal to unity and that is the value for the "actual infinity" used in the present work. The number of nodes along the chord of the airfoil was taken in different experiments between 23 and 49. For the particular airfoil under consideration, its optimal value turned out to be 43. The number of nodes N_W alongside the the cut was taken between 15 and 40. For $x_\infty = 7$ the optimal number appeared to be 20. For $N_W > 20$ the result did not change significantly in comparison with $N_W = 20$, while smaller N_W led to unacceptably rough results.

We have found the solution for both the signs of the radical in eq.(8), but the solution for the positive sign corresponds to the so-called laminar separation and has not practical significance for airfoils. Hence, in the present work we resort to the other case - the negative sign. Following the terminology adopted in our previous works, we call it *solution I*. In Figs. 2 are shown the shapes of the two free boundaries of the separation zone (*solution I*) for angles of attack $\alpha = 8°$ and $\alpha = 16°$

Figs. 3 presents the chord-wise distribution of the surface pressure for the same two cases. For comparison, the experimental data of [13] for $Re = 2.7.10^6$ for the nearest available angle of attack is juxtaposed in Figs. 3. The agreement between the numerical solution and experimental measurements is fully satisfactory.

An important follow-up of our model are the predictions for the forces exerted from the discontinuous flow upon the body (airfoil). For $\alpha = 8°$ we obtained values

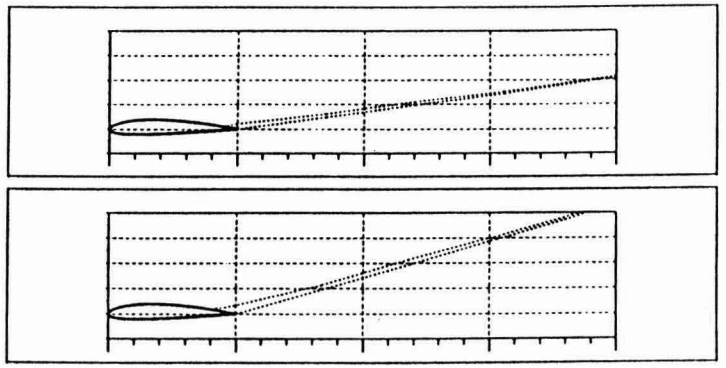

Figure 2: Shape of the separated zone for NACA2412. Up: $\alpha = 8°$; down: $\alpha = 16°$

$C_x = 0.017$ for the drag coefficient and $C_y = 0.9354$ - for the lifting-force coefficient. These results are in 95% agreement with the experimental results [1]. The important point here is that our results were obtained without any fudging parameters and without postulating the presence of a circulation around the airfoil (so-called Kutta-Joukowski postulate). In addition to the delightful prediction for the lifting force, we obtain the drag coefficient, the latter being zero by definition for the models employing the circulation postulate.

Acknowledgment A Sabbatical Fellowship form the Spanish Ministry of Science and Education is gratefully acknowledged by CIC. CIC also acknowledges the hospitality of the Lab. de Mecanique, Université de Caen during the preparation of the manuscript.

References

[1] I. E. Abott and A. E. Doenhoff. *Theory of wing sections.* Dover, 1959.

[2] S. Brodetsky. Discontinuous fluid motion past circular and elliptic cylinders. *Proc. Roy. Soc., London A*, 718:542–553, 1923.

[3] C. I. Christov and M. D. Todorov. Numerical investigation of separated or cavitating inviscid flows. In *Proc. Int. Conf. Num. Methods and Applications, Sofia 1984*, pages 216–233, 1985.

[4] C. I. Christov and M. D. Todorov. On the determination of the shape of stagnation zone in separated inviscid flows around blunt bodies. In *Proc. XV Jubilee Session on Ship Hydrodynamics*, page paper 10, Varna, 1986. BSHC.

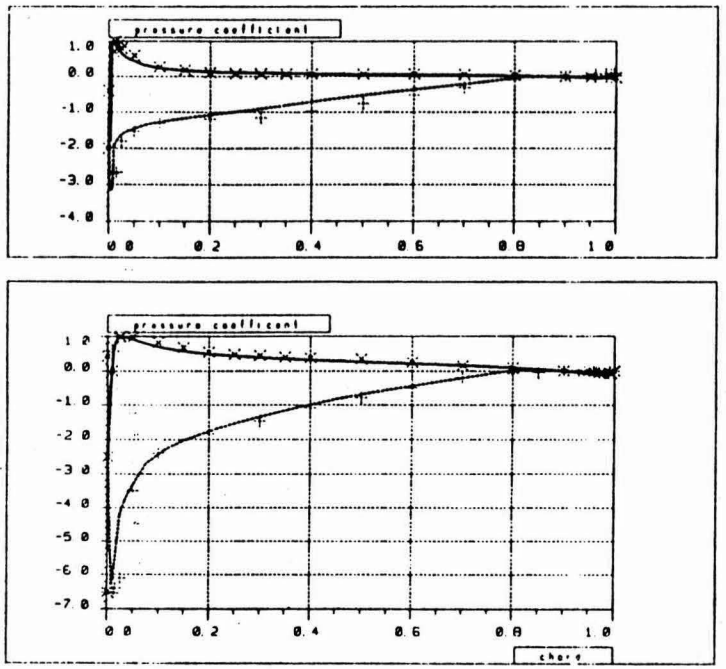

Figure 3: Pressure distribution on the lower and upper surfaces for NACA2412. Up: $\alpha = 8°$; down: $\alpha = 16°$ Lines – the present solution; symbols - $Re = 2.7.10^6$ (Riegels)

[5] C. I. Christov and M. D. Todorov. An inviscid model of flow separation around blunt bodies. *Compt. Rend. Acad. Bulg. Sci.*, 7:43–46, 1987.

[6] C. I. Christov and M. D. Todorov. Numerical solution of 2d Helmholtz problem for blunt bodies and airfoils. In V. V. Kozlov and A. V. Dovgal, editors, *Separated Flows and Jets*, pages 175–180, Berlin, 1990. Springer.

[7] B. Fornberg. A numerical study of steady viscous flow past a circular cylinder. *J. Fluid Mech.*, 98:819–855, 1980.

[8] B. Fornberg. Steady viscous flow past a circular cylinder up to Reynolds number 600. *J. Comput. Phys.*, 61:297–320, 1985.

[9] M. I. Gurevich. *Theory of Jet Flows of Ideal Fluids.* Nauka, Moscow, 1979. in Russian.

[0] H. Helmholtz. Uber discontinuirliche flussigkeitsbewegnungen. *Monatsbericht. d. Akad. d. Wiss.*, (Berlin):215–228, 1868.

[11] G. Kirchhoff. Zur theorie freier flussigkeitsstrahlen. *J. Reine Angew. Math.*, 70:289–298, 1869.

[12] D. H. Peregrine. A note on the steady high-Reynolds-number flow about a circular cylinder. *J. Fluid Mech.*, 157:493–500, 1985.

[13] F. Riegels. *Aerodynamische Profile.* Oldenbourg, Munchen, 1958.

[14] F. T. Smith. A structure for laminar flow past a bluff body at high Reynolds number. *J. Fluid Mech.*, 155:175–191, 1985.

[15] M. D. Todorov. Christov's algorithm for Helmholtz problem: an integral-equations implementation. In *Proc.XVIII National Summer School "Application of Mathematics in Technology", Varna, 25.8.-2.9.1992*, pages 191–193, Sofia, 1993.

[16] M. D. Todorov and C. I. Christov. Application of the model of inviscid separation for investigation of flows around airfoils. *Ann. Univ. Sof., Fac. Math. & Inform.*, 82 (Book 2 - Mechanics):193–217, 1988. In Russian.

[17] H. Villat. *Sur la resistance des fluides, Apercus theoriques.* Number No 38. Gauthier-Villars, Paris, 1920.

M. D. Todorov
Dept. Diff. Equations, Institute of Applied Mathematics & Informatics,
Technical University, Sofia 1156, BULGARIA

C. I. Christov
Instituto Pluridisciplinar, Universidad Complutense,
Paseo Juan XXIII, No 1, 28040, Madrid, SPAIN